

Analyzing C-SPSWs with outriggers for tall buildings under lateral loads

Cigdem Avci-Karatas

*Department of Transportation Engineering, Faculty of Engineering, Yalova University,
77200, Yalova, Turkey
cigdem.karatas@yalova.edu.tr*

ABSTRACT

Structures that are tall and short are designed and perform differently. Different approaches are presented to tall and short structures for resisting gravity and lateral loads. For tall structures, providing appropriate stiffness and strength, as well as the required yielding capacity, differs greatly from short structures. An analytical study was conducted in this study to determine how a coupled steel plate shear wall (C-SPSW) and outriggers influence the behavior of tall buildings. A combination of outriggers and C-SPSWs provides a strong and durable system with extremely high shear and bending rigidity. There are many tedious calculations that have to be made in order to determine the optimal location of an outrigger. This considered study centered on obtaining the equations that govern the behavior of the proposed combined system and determining the optimal locations for the outriggers on tall buildings with any number of stories. Equations proposed by the paper agree well with the results of a finite element model (FEM). The results show that the location of an outrigger is more important than its rigidity. Furthermore, this study indicates that column rigidity does not have a significant effect on lateral deformations. Also, by increasing the rigidity of beams, the lateral movement of a building structure is reduced.

Keywords: Outrigger; Steel plate shear wall (SPSW); Coupled wall; Drift; Stiffness; Strength; Seismic protection technology.

1. INTRODUCTION

There are differences in the design and performance of tall and short structures. Therefore, the tall and short structures require different stiffening systems to resist gravity and lateral loads. So, a tall structure requires different stiffness and strength criteria than a short structure, as well as different yielding capacities. Short buildings usually do not have a problem with drift control, and most control issues can be handled by the forces that determine how the structure behaves. However, one of the biggest (or most important) design challenges in tall buildings is to control lateral displacements.

Structures have been controlled using a number of different methods (Qu and Xu 2001; Esmaeili *et al.* 2013) which can be broken down into active, passive, and semi-active mechanisms. In tall buildings, using a shear wall is an appropriate way to control shear displacement. Even so, the shear wall has no significant influence on the bending displacement of the structure. In this respect, an outrigger could be used to prevent the bending displacement of a tall building.

Steel plate shear walls (SPSWs), especially coupled steel plate shear walls (C-SPSWs) have not been adequately studied, despite valuable research on concrete shear walls. In the case of two coplanar shear walls connected by simple joints (which can only transfer axial forces between the walls), the moments applied to each wall are separately resisted by the internal moments of both. A wall's bending stiffness is directly related to the amount of internal moments. The internal moments in each wall result in linear distribution of flexural stresses along each wall, with maximum tensile and compressive stresses appearing along the edges of each wall. For example, in the case where the walls are joined by rigid beams, they form a double vertical cantilever, which permits the applied moments to be tolerated by both walls (which behave as one integrated system) by bending about the central axis of the integrated system. In this state, the flexural stresses are distributed linearly along with the integrated system, with the maximum tensile and compressive stresses accumulating at the two ends of the wall (Fig. 1).

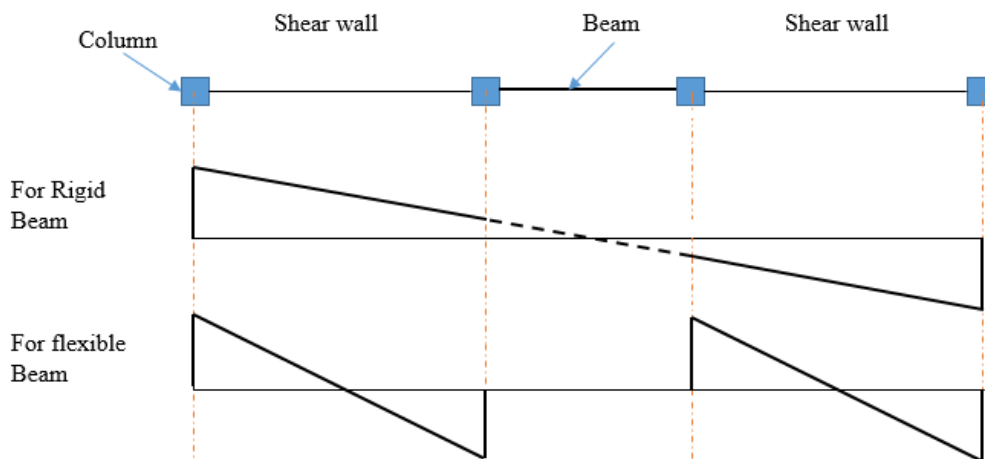


Fig. 1 Comparison of the stresses between two types of beam between C-SPSWs

In this system, two walls are joined by flexible beams that behave somewhere between a completely rigid state and a fully flexible connection. Coupled shear walls are characterized by two states. If the beams are rigid, the structure will behave like a cantilever. In recent years, researchers have demonstrated that coupled shear walls behave differently from ordinary shear walls, and that their lateral deformation increases hyperbolically with height (Chan and Kuang 1989). When a C-SPSW is used, its stiffness value exceeds that of the two constituent walls together (Timler and Kulak 1983; Astaneh-Asl 2001); as a result, the system performs better. In experimental works, SPSWs have exhibited satisfactory behavior (Hatami *et al.* 2014; Zhou *et al.* 2010; Hosseinzadeh *et al.* 2017a; Hosseinzadeh *et al.* 2017b). By presenting the relevant

*The 2022 World Congress on
The 2022 Structures Congress (Structures22)
16-19, August, 2022, GECE, Seoul, Korea*

equations for estimating the lateral deformations of a steel shear wall, many researchers (Vetr *et al.* 2016; Hoenderhamp 2011; Coull and Bensmail 1991) have demonstrated that this system has high stiffness, yielding capacity, and resistance against lateral loads.

In tall structures, SPSWs are an economically viable alternative to concrete shear walls due to their low thickness, their ease of erection process, and their satisfactory performance. Despite this, the behavior of a C-SPSW has received less research than that of a conventional SPSW. As a building's height increases, the effect of bending displacements on the structure's behavior will increase, and this will be challenging to control. SPSW have high shear stiffness, which makes them able to withstand shear loads. Columns of tall buildings are subjected to enormous forces as a result of displacements and overturning moments. Many high-rise buildings in the world use outriggers to reduce these forces. Combining SPSW and outriggers can provide a good system for dealing with displacements caused by shear or bending. Research has shown that the integrated behavior of building core and outrigger can be predicted by design equations (Coull and Bensmail 1991; Taranath 2012). For use in tall buildings, however, the equations for the outrigger and steel coupled shear wall have not been presented yet. Taranath (2012) has demonstrated that by using an outrigger, building stiffness increases by about 25% to 30%. Also, the optimal height for a single outrigger is roughly at the midpoint of a structure (45.5% of building height from the top). Despite the outrigger system's increases in bending stiffness, it has little effect on shear strength, since the majority of shear is absorbed by the core (Broujerdian *et al.* 2016; Broujerdian *et al.* 2017). The current study investigated the combined system of a single outrigger and C-SPSW, presenting the mathematical equations for this system as well as the optimal outrigger location.

2. C-SPSW ANALYSIS

To analyze the buildings that contain coupled shear walls, several known methods including the continuum method and the wide column method are employed (Broujerdian *et al.* 2016). In the continuum approach of structural analysis, the beams of the coupled wall are replaced by uniform shears along with the height. It is also assumed that both walls at a level deform together. Thus, the inflection point occurs in the middle of the coupled beams. Consider an outrigger at height h_s (Fig. 2). The separate set of axial force, shear force, and bending moments of the coupled beams can be replaced by equivalent continuous distribution and load intensity per unit height. The continuum and its simplified parameters have been illustrated in Figs. (3) and (4).

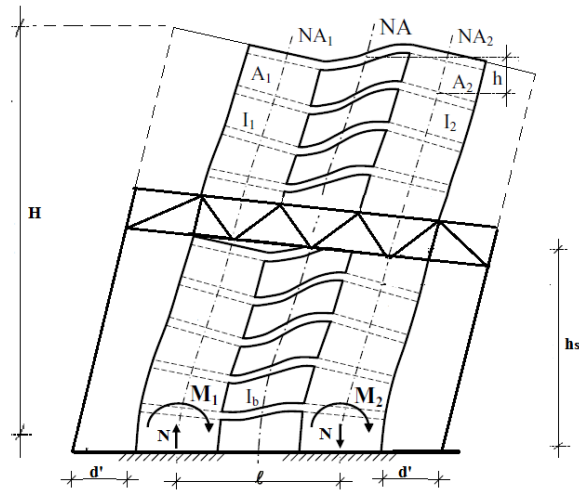


Fig. 2 Combination of a coupled shear wall and an outrigger

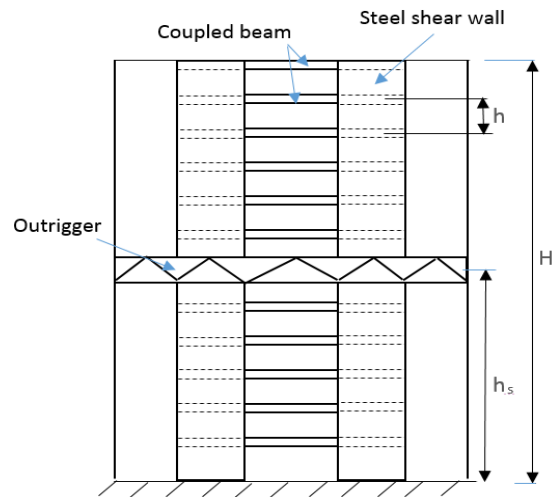


Fig. 3 Specifications of a combined system of C-SPSW and outrigger

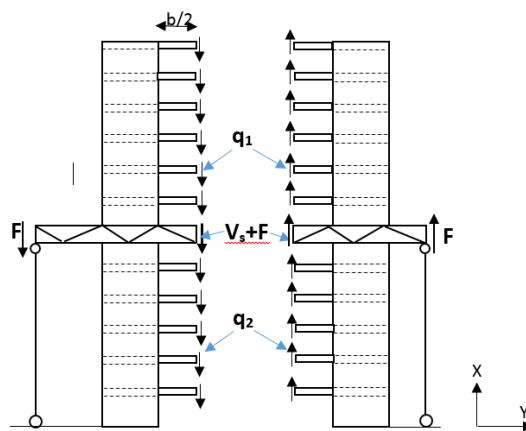


Fig. 4 Internal forces in a combined system of C-SPSW and outrigger

The 2022 World Congress on
The 2022 Structures Congress (Structures22)
 16-19, August, 2022, GECE, Seoul, Korea

If the structure is cut into half along the vertical direction and at the midpoints of coupled beams (the locations of bending inflection points), its internal forces will include the shear force with magnitude $q(x)$ per unit height and axial force with magnitude $n(x)$ per unit height (Fig. 4). Thus, axial force N at each wall level will be obtained by integrating the shear above that level.

$$N = \int_x^H q dx \quad (1)$$

$$q = -\frac{dN}{dx} \quad (2)$$

By considering the top and bottom of an outrigger, the axial force of each wall will be:

$$N_1 = \int_x^H q_1 dx \quad (3)$$

$$N_2 = \int_z^H q_1 dx + V_s + \int_x^z q_2 dx \quad (4)$$

If the compatibility conditions along the vertical directions of bending inflection points are considered, due to the four types of behaviors shown below, the relative vertical displacements at the ends of the parallel cantilevers will be displayed according to Fig. 5. These four types of displacements are:

1) Wall rotation due to bending (Fig. 5a), which produces a relative vertical displacement and is equal to:

$$\delta_1 = \left(\frac{b}{2} + d_1\right) \frac{dy}{dx} + \left(\frac{b}{2} + d_2\right) \frac{dy}{dx} = l \frac{dy}{dx} \quad (5)$$

In this equation, $\frac{dy}{dx}$ is the slope of a wall's central axis at level x and it is due to combined bending.

2) Shear and bending displacement of coupled beams due to the applied shear (Fig. 5b), which is expressed as:

$$\delta_2 = \frac{hb^3}{12EI_b} \frac{dN}{dx} \quad (6)$$

3) Axial deformation of walls due to the axial force N (Fig. 5c), which is caused by the shear force applied to the coupled beams (the sum of the shears in coupled beams will be equal to the axial force). The deformation below the outrigger level differs from that above the outrigger, and it is equal to:

$$\delta_3 = \int_0^x N dx = \frac{2}{EA} \left[\int_z^x N_1 dx + \int_0^z N_2 dx \right] \quad (7)$$

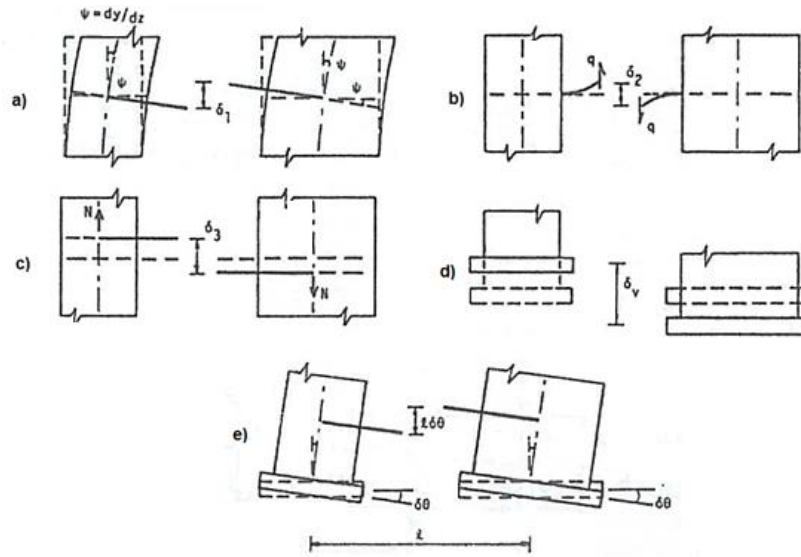


Fig. 5 Relative vertical displacements in the coupled beam

4) The vertical deformation or the rotation of the wall base, δ_4 , when the wall is fixed to the foundation, will be equal to zero. In the primary deformed structural system of **Fig. 1**, no relative vertical displacement exists at the bending inflection points of coupled beams. Thus, the vertical compatibility conditions at this state require the following relation to be true:

$$\delta_1 + \delta_2 + \delta_3 + \delta_4 = 0 \quad (8)$$

In other words, by considering the location of an outrigger, we will have:

$$l \frac{dy_1}{dx} - \frac{hb^3}{12EI_b} q_1 - \frac{2}{EA} \left[\int_z^x N_1 dx + \int_0^z N_2 dx \right] = 0 \quad (9)$$

$$l \frac{dy_2}{dx} - \frac{hb^3}{12EI_b} q_1 - \frac{2}{EA} \int_0^x N_2 dx = 0 \quad (10)$$

where I_b , A , and E are the moment of inertia of the coupled beams, the cross-sectional area of the steel shear wall, and the elasticity modulus of the shear wall, respectively. By considering the bending due to the external moment M and the reverse bending moment resulting from the shear and axial forces at the bending moment inflection points (where the structure has been split (**Fig. 5**)), the moment-curvature equations for each level and both walls above and below the outrigger will be:

$$\begin{cases} M = EI \frac{d^2 y_1}{dx^2} + N_1 l \\ M = EI \frac{d^2 y_2}{dx^2} + N_2 l \end{cases} \quad (11)$$

The 2022 World Congress on
The 2022 Structures Congress (Structures22)
 16-19, August, 2022, GECE, Seoul, Korea

By taking a derivative from Eqs. 9 and 10 and combining them with Eqs. 11, the curvature $\frac{d^2y}{dx^2}$ will be eliminated and the final outcome will become:

$$\frac{d^2N_1}{dx^2} - (\alpha\gamma)^2 N_1 = -\frac{\gamma^2}{l} M \quad (12)$$

$$\frac{d^2N_2}{dx^2} - (\alpha\gamma)^2 N_2 = -\frac{\gamma^2}{l} M \quad (13)$$

Assuming that a steel shear wall behaves like a cantilever plate girder, the columns around the steel shear wall act like the flanges of the girder; and at the considered level, they have the same cross-section. Considering the small thickness of the plate, it can be ignored in computing the moment of inertia of the steel shear wall. So, with good accuracy, the moment of inertia of each steel shear wall can be expressed as:

$$I_1 = 2A_c \left(\frac{l_w}{2}\right)^2 = \frac{A_c l_w^2}{2} \quad (14)$$

where A_c is the cross-sectional area of the columns around the steel plate. If the moments of inertia of the two walls are assumed to be equal, $I = 2I_1$, we will have:

$$I = A_c l_w^2 \quad (15)$$

$$\frac{\gamma}{\alpha^2} = \frac{l}{l^2 + l_w^2 \frac{A_c}{A}} \quad (16)$$

$$\alpha^2 = \frac{6I_b}{hb^3 A_c} \left(\left(\frac{l}{l_w}\right)^2 + \frac{A_c}{A} \right) \quad (17)$$

$$\gamma = \frac{6I_b l}{hb^3 A_c l_w^2} \quad (18)$$

The left sides of Eqs. (12) and (13) indicate the physical specifications of a structure, and their right sides express the type of the applied force. To obtain the shear force (V_s) in the coupled beams, by applying the compatibility conditions at the turning points we get:

$$l \frac{dy_2}{dx} - \frac{V_s b^3}{12E_s I_s} - \frac{2}{EA} \int_0^{h_s} N_2 dx = 0 \quad (19)$$

In this equation, $E_b I_b$ denotes the bending stiffness of the coupled beams. By inserting Eq. 9 or Eq. 10 into Eq. 19 and considering $K_0 = \frac{h E_s I_s}{H E I_b}$ (the relative bending stiffness of coupled beams), the shear force in the coupled beams at level h_s is obtained.

$$V_s = K_0 H q_{1s} = K_0 H q_{2s} \quad (20)$$

3. EFFECTS OF THE OUTRIGGER AND THE EXTERNAL LOAD

An outrigger increases the bending stiffness of a structure but does not affect on its shear stiffness. Because of the high shear stiffness of the steel shear wall, this system will not suffer from a shortage of shear stiffness. Therefore, the combination of these two systems shall behave satisfactorily. The bending moment M_h in the outrigger is defined as:

$$M_h = Fd \quad (21)$$

By considering M_h , the external bending moment in Eqs. (12) and (13) is obtained.

$$\begin{cases} M = 0; & hs \leq x \leq H \\ M = M_h; & hs \leq x \leq H \end{cases} \quad (22)$$

Thus, the general solutions of Eqs. (7) and (8) are written as:

$$N_{1M} = B_1 \cosh \alpha x + C_1 \sinh \alpha x \quad (23)$$

$$N_{2M} = B_2 \cosh \alpha x + C_2 \sinh \alpha x + \frac{l}{l^2 + l_w \frac{2A_c}{A}} M_h \quad (24)$$

The values of shear per unit length at the top and bottom of the outrigger, obtained from Eq. 2, are as follows:

$$q_{1M} = -[B_1 \alpha \sinh \alpha x + C_1 \alpha \cosh \alpha x] \quad (25)$$

$$q_{2M} = -[B_2 \alpha \sinh \alpha x + C_2 \alpha \cosh \alpha x] \quad (26)$$

Under the external load, the applied moment can be expressed as:

$$M = M_l = \frac{w}{2} (H - x)^2 \quad (27)$$

and by solving Eqs. (7) and (8), the axial forces at the top and bottom of the outrigger, with a uniform load intensity (w) along the wall height, are respectively obtained as:

$$N_{1l} = B'_1 \cosh \alpha x + C'_1 \sinh \alpha x + \frac{l}{l^2 + l_w \frac{2A_c}{A}} (M_l + \frac{w}{\alpha^2}) \quad (28)$$

$$N_{2l} = B'_2 \cosh \alpha x + \frac{\gamma \cdot w \cdot H}{\alpha^2} \sinh \alpha x + \frac{l}{l^2 + l_w \frac{2A_c}{A}} (M_l + \frac{w}{\alpha^2}) \quad (29)$$

Also, the amount of shear at the bending moment inflection points, arising from an external load, is equal to:

$$q_{1l} = -[B'_1 \alpha \cosh \alpha x + C'_1 \alpha \sinh \alpha x + \frac{l}{l^2 + l_w \frac{2A_c}{A}} (\frac{dM_l}{dx})] \quad (30)$$

The 2022 World Congress on
The 2022 Structures Congress (Structures22)
 16-19, August, 2022, GECE, Seoul, Korea

$$q_{2l} = -[B'_2 \alpha \sinh \alpha x + C'_2 \alpha \cosh \alpha x + \frac{l}{l^2 + l_w^2 \frac{A_c}{A}} \left(\frac{dM_l}{dx} \right)] \quad (31)$$

In the above equations, the values of B_1 , B_2 , C_1 , and C_2 can be obtained by applying the boundary conditions. At the top of the structure, where $x = H$, we will have:

$$N_1(H) = 0 \quad (32)$$

The boundary conditions at the level h_s are as follows:

$$N_1(z) + V_s + F_i = N_2(z) \quad (32)$$

$$q_1(h_s) = q_2(h_s) \quad (33)$$

$$q_2(0) = 0 \quad (34)$$

Also, the amount of shear at the structure base is equal to:

$$B_1 = -C_1 \tanh \alpha H \quad (35)$$

$$B_2 = -C_1 \left(\frac{1}{\tanh \alpha h_s} - \tanh \alpha h \right) \quad (36)$$

$$C_2 = 0 \quad (37)$$

$$C_1 = \frac{\left(\frac{-1}{d} + \frac{d'}{a^2} \right) M_h}{(-K_2 \tanh \alpha H + K_3 - \frac{\cosh \alpha z}{\tanh \alpha z} + \cosh \alpha h_s (\tanh \alpha z))} \quad (38)$$

By considering **Eq. 4**:

$$N_1(z) + V_s = N(z) \quad (39)$$

Moreover, constants B'_1 , B'_2 , C'_1 , and C'_2 , can also be obtained:

$$C'_1 = \frac{\tanh \alpha h_s (B'_2 - K_1) - C_2}{1 - \tanh \alpha h_s \tanh \alpha H} \quad (40)$$

$$B'_1 = K_1 - C'_1 \tanh \alpha H \quad (41)$$

$$B'_2 = \frac{(K_1 K_2 - K_4 C'_2 \tanh \alpha h_s) + K_1 \tanh \alpha h_s - C_2}{\cosh \alpha h_s + \frac{K_5 \tanh \alpha h_s}{1 - \tanh \alpha h_s \tanh \alpha H}} \quad (42)$$

The constants used in calculating B'_1 , B'_2 , C'_1 and C'_2 are as follows:

$$K_1 = \frac{-\gamma w}{\alpha^4 \cosh \alpha H} \quad (43)$$

$$K_2 = \cosh \alpha h_s - K_0 \sinh \alpha h_s \quad (44)$$

$$K_3 = \text{Sinh } \alpha h_s - K_0 \alpha H \cosh \alpha h_s \quad (45)$$

$$K_4 = K_0 \frac{\gamma}{\alpha^2} [w \cdot H(H - h_s)] \quad (46)$$

$$K_5 = K_2 \tanh \alpha H - K_3 \quad (47)$$

4. EQUATIONS FOR OBTAINING THE LATERAL DEFORMATIONS

By twice integrating Eq. 3 and using the compatibility conditions in Eqs. (48) and (49) and also the boundary conditions in Eqs. (50) and (51), the lateral deformations due to the outrigger and external load are obtained.

$$y_2(0) = 0 \quad (48)$$

$$y'_2(0) = 0 \quad (49)$$

$$y_1(z) = y_2(z) \quad (50)$$

$$y'_1(z) = y'_2(z) \quad (51)$$

The lateral deformation due to the outrigger can be determined from the following equations:

$$y_{1M} = -\frac{1}{EA_c l_w^2} \left[\frac{C_1}{\alpha^2} (l \sinh \alpha x - \tanh \alpha H l \cdot \cosh \alpha x) + x K_6 + K_7 \right] \quad (52)$$

$$y_{2M} = -\frac{1}{EA_c l_w^2} \left[\left(1 - \frac{1}{1 + \left(\frac{l_w}{l}\right)^2 \frac{A_c}{A}} \right) M_h x^2 + \frac{C_1 \left(\frac{1}{\tanh \alpha z} - \tanh \alpha h \right) l}{\alpha^2} \cosh \alpha x + \frac{l B_2}{\alpha^2} \right] \quad (53)$$

Coefficients K_6 and K_7 in the above equations are obtained as:

$$K_6 = - \left[\left(\frac{l}{l^2 + l_w^2 \frac{A_c}{A}} \right) M \cdot z + (B_1 - B_2) \frac{l}{\alpha} \sinh \alpha z + \frac{C_1}{\alpha^2} \cos \alpha z \right] \quad (54)$$

$$K_7 = - \left[0.5 \left(1 - \frac{1}{1 + \left(\frac{l_w}{l}\right)^2 \frac{A_c}{A}} \right) M \cdot z^2 + (B_1 - B_2) \frac{l}{\alpha^2} \sinh \alpha z + \frac{l C_1}{\alpha^2} \cos \alpha z + \delta_1 z + \frac{l B}{\alpha^2} \right] \quad (55)$$

where l is the center-to-center distance between the shear walls. The lateral deformation due to the lateral load is equal to:

$$y_{1l} = -\frac{1}{EA_c l_w^2} \left[\left(1 - \frac{1}{1 + \left(\frac{l_w}{l}\right)^2 \frac{A_c}{A}} \right) A(x) - \frac{1}{\alpha} B(x) + \frac{1}{\alpha^2} C(x) - \frac{1}{1 + \left(\frac{l_w}{l}\right)^2 \frac{A_c}{A}} \left(\frac{w x^2}{2 \alpha^2} \right) \right] \quad (56)$$

In this equation, coefficients $A(x), B(x), C(x)$ are expressed as follows:

The 2022 World Congress on
The 2022 Structures Congress (Structures22)
 16-19, August, 2022, GECE, Seoul, Korea

$$A(x) = \frac{w}{24}(x^4 - 4Hx^3 + 6H^2x^2) \quad (57)$$

$$B(x) = [(B'_1 - B'_2)\sinh\alpha z + (C'_1 - C'_2) \cosh\alpha z](x - z) \quad (58)$$

$$C(x) = B'_1(\cosh\alpha z - \cosh\alpha z) + C'_1(\sinh\alpha z - \sinh\alpha z) + B'_2(1 - \cosh\alpha z) + C'_2(\alpha x - \sinh\alpha z) \quad (59)$$

Thus, we have:

$$y_{2l} = -\frac{1}{EA_c l_w^2} \left[\left(1 - \frac{1}{1 + \left(\frac{l_w}{l}\right)^2 \frac{A_c}{A}} \right) A(x) - \frac{1}{\alpha} D(x) + \frac{1}{1 + \left(\frac{l_w}{l}\right)^2 \frac{A_c}{A}} \left(\frac{wx^2}{2\alpha^2} \right) \right] \quad (60)$$

where $A(x)$ is defined based on [Eq. 57](#) and parameter $D(x)$ is expressed as:

$$D(x) = B'_2(1 - \cosh\alpha x) + C'_2(\alpha x - \sinh\alpha x) \quad (61)$$

To verify the proposed equations, a 21-story building structure (height of each story = 3.2 m) has been considered and an outrigger has been placed at the 11th story (mid-height of the structure). This building has been subjected to a uniform distributed load. The geometrical specifications and mechanical properties of the structure have been selected such that $l = \frac{l_w}{50} \sqrt{\frac{hb^3 A_c}{I_b} - \frac{A_c}{A}}$. Thus, based on [Eqs. \(16\) through \(19\)](#), constants ω and ψ are obtained as $5.2 \exp^{-5}$ and 0.133, respectively. The structure has been analyzed in the ANSYS software environment by the FEM and also using the equations proposed in this work. The roof displacement obtained by FEM was 10.790 mm, while the proposed equations estimated the roof displacement as 10.839 mm. This indicates that the proposed equations are highly accurate and can be used in practical design procedures. It was demonstrated that the mid-height of a building structure is the optimal location for an outrigger.

5. MODELING

To study the effect of the rigidity of a system's constituent elements on a drift, with the outrigger installed at the mid-height, several models were analyzed through FEM, and their results were evaluated. By knowing how the rigidity of a member affects the behavior of a structure, a designer can make the right decision to increase or reduce the rigidity of each element in the preliminary or even in the final design. In this regard, thirty 31-story building structures with the height of each story being 3 m and the span width (axis-to-axis distance between columns) being 5 m were modeled and analyzed. These structures were subjected to uniformly distributed loads and the same load intensity. The structures were designed so that the ratios of beam-to-column, outrigger-to-shear wall, and shear wall-to-bending frame rigidities are all equal to one. The consideration of equal rigidities was to facilitate the comparing of the systems and to determine the effect of each component's rigidity on the behavior of a structure. Thus, a structure with the same rigidity for all its elements is designated by $EI = 1$. The number after the equal sign

The 2022 World Congress on
The 2022 Structures Congress (Structures22)
16-19, August, 2022, GECE, Seoul, Korea

indicates the rigidity factor of a structure. For example, $EI = 100$ means that the structure rigidity has increased 100 times. Fig. 6 shows the effects of a single outrigger, combined system of shear wall, and outrigger and the bending frame system on drift ratio.

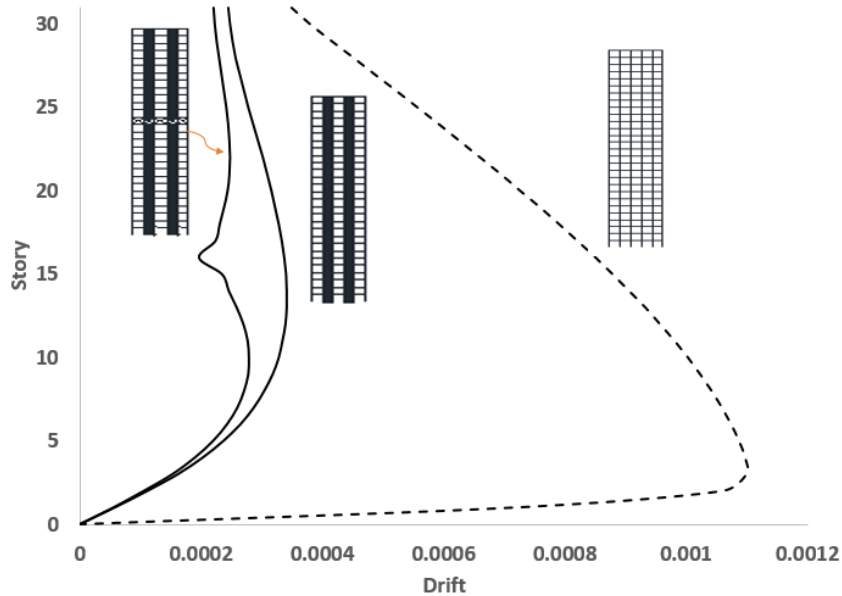


Fig. 6 Effects of different systems on drift ratio

The location of an outrigger is much more important than the rigidity of its members. By comparing Fig. 7 it can be realized that, with the increase of outrigger rigidity, the drift ratio diminishes, but not very much.

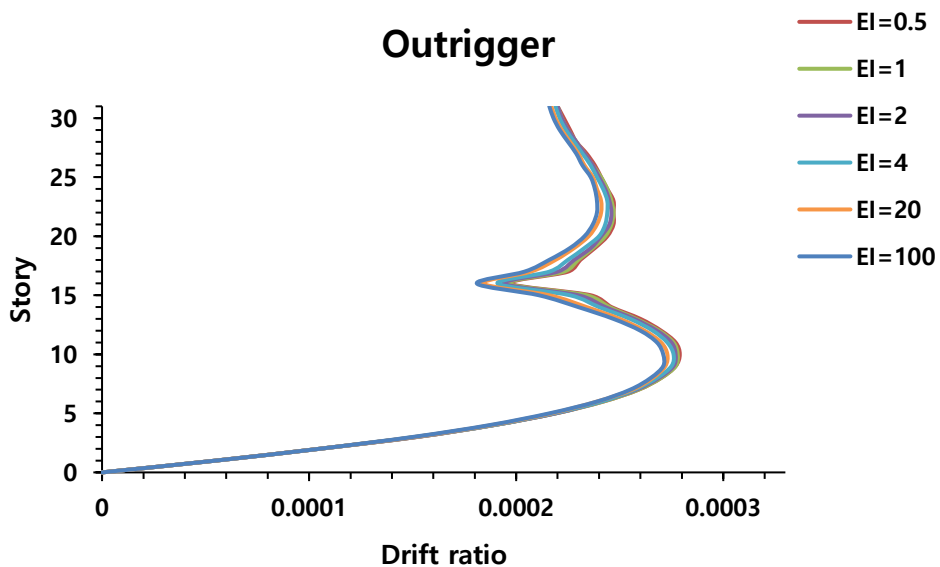


Fig. 7 Effect of outrigger rigidity on drift ratio

By examining Fig. 8 it is observed that the drift ratio diminishes with the increase of shear wall thickness.

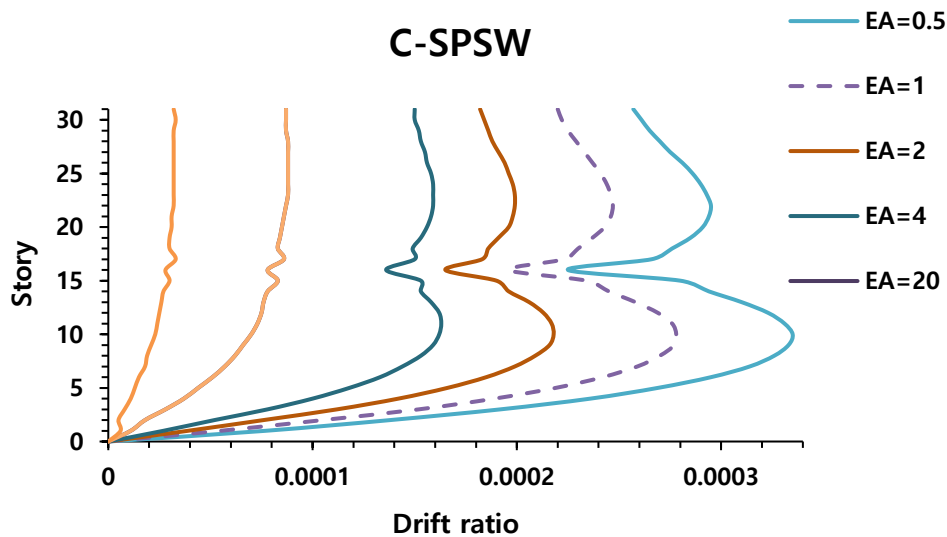


Fig. 8 Effect of C-SPSW rigidity on drift ratio

If the rigidity of beams is increased and the other parameters are kept constant, the drift ratio values will be reduced (Fig. 9). Contrary to beams and walls, which considerably reduce the lateral displacement of a structure as their rigidity increases, columns do not follow the same trend; because by increasing the moment of inertia of columns, the effect of the beams is reduced and the columns independently resist the lateral loads. Now, in high-rise buildings, even if the rigidity of columns becomes 100 fold, the structure will not be rigid, and its rigidity will be less than the rigidity of a structure equipped with outriggers. This fact can be observed in Fig. 10; because if column rigidity was to reduce the effect of the outrigger, the drift ratio of the 16th story shouldn't have diminished suddenly. Therefore, the increase of column rigidity will have a negligible effect on the controlling of lateral displacements; because column rigidity will be meaningful in conjunction with the ratio of beam-to-column moment of inertia.

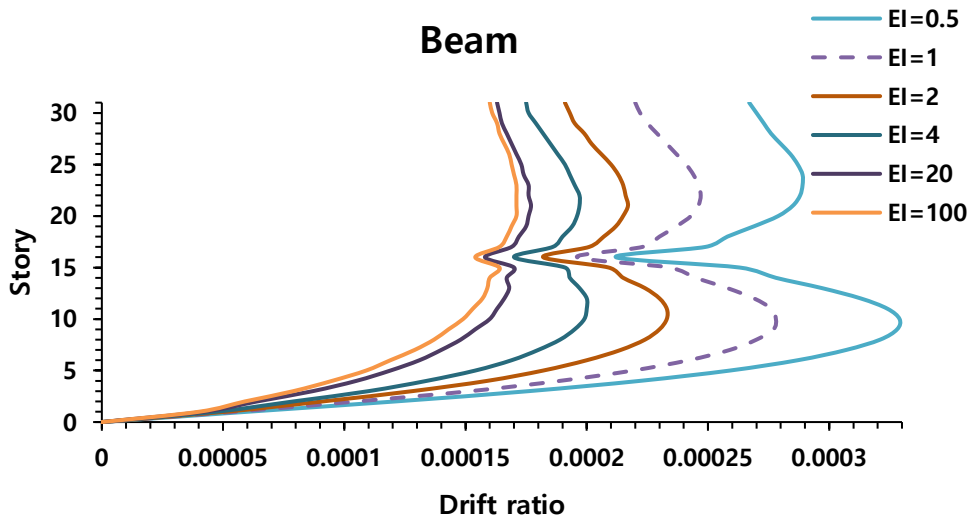


Fig. 9 : Effect of beam rigidity on drift ratio

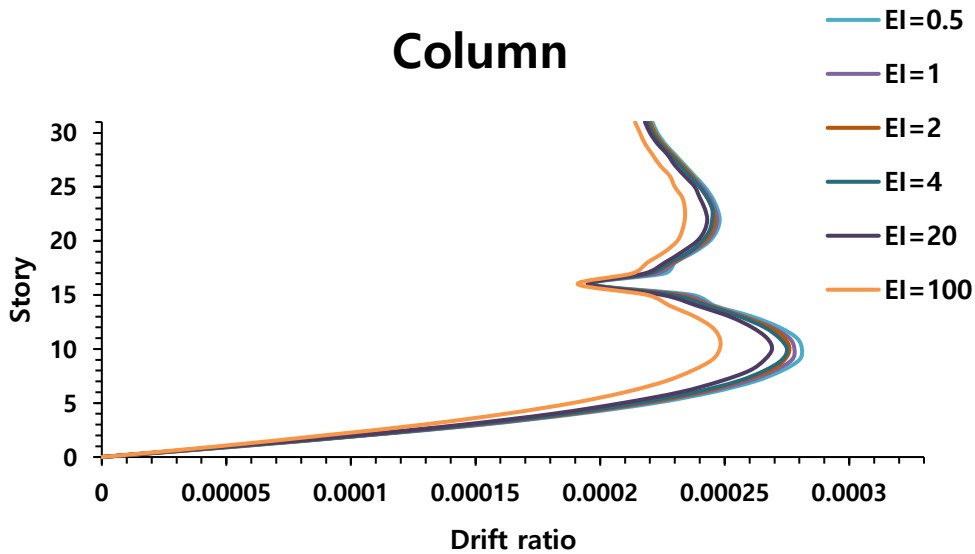


Fig. 10 : Effect of column rigidity on drift ratio

6. CONCLUSIONS

In this paper, an analysis of the deflection of lateral displacements of a tall building structure has been conducted numerically and parametrically with an outrigger and C-SPSW system combined. According to this study, location is far more important than rigidity in determining the performance of an outrigger. An outrigger's configuration and geometry enable it to function as a rigid element inherently. The displacement equation

*The 2022 World Congress on
The 2022 Structures Congress (Structures22)
16-19, August, 2022, GECE, Seoul, Korea*

was plotted in this research to make it easier to use the complicated structural deformation equation. According to this diagram, the closer an outrigger is to the mid-height of a building, the more effective it will be. An outrigger's efficiency is reduced to a minimum when it is placed at a height where the ratio is low. As the rigidity of beams increases, the displacement and drift values of a building will decline less than a certain limit. However, increasing beam rigidity to infinity will not cause the displacement and drift values to decrease to zero. Further, as beam rigidity increases, the effect of an outrigger on drift diminishes, since each story's rigid beam acts as an outrigger. Unlike beams, columns are not significantly less prone to lateral displacements as rigidity is increased.

REFERENCES

- Astaneh-Asl, A., (2001), "Seismic Behavior and Design of Steel Shear Walls-SEONC Seminar", Paper Distributed and presented at the 2001 SEOANC Seminar, Structural Engineers Assoc. of Northern California, November 7, 2001, San Francisco. <http://faculty.ce.berkeley.edu/astaneh/>.
- Broujerdian, V. Ghamari, A. Ghadami, A. (2016), "An investigation into crack and its growth on the seismic behavior of steel shear walls," *Thin-Walled Struct.*, **101**, 205–212. <https://doi.org/10.1016/j.tws.2015.09.016>.
- Broujerdian, V. Shayanfar, M. Ghamari, A. (2017), "Corner crack effect on steel plate shear wall," *Civ. Eng. Infrastruct. J.*, **50**(2), 311–332. <https://doi.org/10.7508/CEIJ.2017.02.007>.
- Chan, H.C., Kuang, J.S. (1989), "Stiffened coupled shear walls," *J. Eng. Mech. (ASCE)*, **115**(4), 689–703. [https://doi.org/10.1061/\(ASCE\)0733-9399\(1989\)115:4\(689\)](https://doi.org/10.1061/(ASCE)0733-9399(1989)115:4(689)).
- Coull, A., Bensmail, L. (1991), "Stiffened coupled shear walls," *J. Struct. Eng. (ASCE)*, **117**(8), 2205–2223. [https://doi.org/10.1061/\(ASCE\)0733-9445\(1991\)117:8\(2205\)](https://doi.org/10.1061/(ASCE)0733-9445(1991)117:8(2205)).
- Esmaeili, H., Kheyroddin, A., Kafi, M.A., Nikbakht, H. (2013), "Comparison of nonlinear behavior of steel moment frames accompanied with RC shear walls or steel bracings," *Struct. Des. Tall Spec. Build.*, **22**(14), 1062–1074. <https://doi.org/10.1002/tal.751>.
- Hatami, F., Ghamari, A. Hatami, F. (2014), "Effect of fiber angle on LYP steel shear walls behavior," *J. Cent. South Univ.*, **21**, 768–774. <https://doi.org/10.1007/s11771-014-2000-x>.
- Hoenderkamp, J.C.D. (2011), "The influence of single shear walls on the behaviour of coupled shear walls in high-rise structures," *Procedia Eng.*, **14**, 1816–1824. <https://doi.org/10.1016/j.proeng.2011.07.228>.
- Hosseinzadeh, L., Emami, F., Mofid, M. (2017a), "Experimental investigation on the behavior of corrugated steel shear wall subjected to the different angle of trapezoidal plate," *Struct. Des. Tall Spec. Build.*, **26**(17). <https://doi.org/10.1002/tal.1390>.
- Hosseinzadeh, L., Emami, F., Mofid, M. (2017b), "Elastic interactive buckling strength of corrugated steel shear wall under pure shear force," *Struct. Des. Tall Spec. Build.*, **26**(8). <https://doi.org/10.1002/tal.1390>.
- Qu, W.L., Xu, Y.L. (2001), "Semi-active control of seismic response of tall buildings with podium structure using ER/MR dampers," *Struct. Des. Tall Spec. Build.*, **10**(3), 179–192. <https://doi.org/10.1002/tal.177>.
- Taranath, B.S. (2012), "Structural Analysis and Design of Tall Buildings: Steel and Composite Construction," 1st Edition, ISBN 9781439850893, Taylor & Francis Group, LLC CRC Press.
- Timler, P.A., Kulak, G.L. (1983), "Experimental study of steel plate shear walls," Structural engineering report SER 114 | SER-ID SER114. Edmonton (AB): Department of Civil Engineering, University of Alberta. <https://doi.org/10.7939/R3C24QV49>.

*The 2022 World Congress on
The 2022 Structures Congress (Structures22)
16-19, August, 2022, GECE, Seoul, Korea*

- Vetr, M.G., Shirali, N.M., Ghamari, A. (2016), "Seismic resistance of hybrid shear wall (HSW) systems," *J. Constr. Steel Res.*, **116**, 247–270. <https://doi.org/10.1016/j.jcsr.2015.09.011>.
- Zhou, Y., Lu, X., Dong, Y. (2010), "Seismic behavior of composite shear walls with multi-embedded steel sections. Part I: experiment," *Struct. Des. Tall Spec. Build.*, **19**(6), 618–636. <https://doi.org/10.1002/tal.597>.